Appendix Q - Finite Element Analysis of Barrier Pillar Mining at Crandall Canyon Mine

by
William G. Pariseau
University of Utah

FINITE ELEMENT ANALYSIS OF BARRIER PILLAR MINING AT CRANDALL CANYON

Prepared for the Mine Safety and Health Administration
Arlington, Virginia

by

William G. Pariseau

University of Utah
Salt Lake City, Utah

May 26, 2008

CONTENTS

INTRODUCTION

This report discusses finite element analysis of mining in barrier pillars at the Crandall Canyon Mine in central Utah. Analyses are two-dimensional and represent vertical cross-sections from surface to about 1,000 ft (300m) below the mining horizon, the Hiawatha seam. The finite element program is UT2. This computer code has been in service for many years and well validated through numerous bench-mark comparisons with known problem solutions. UT2 has been used in many rock mechanics studies through the years, most recently in the study of inter-panel barrier pillars used in some Utah coal mines.

The study objective is to develop a better understanding of the strata mechanics associated with recent events (August, 2007) at the Crandall Canyon Mine. This mine is in the Wasatch coal field in central Utah, west of Price, Utah. There are three coal seams of interest in the stratigraphic column of the Wasatch Plateau, namely the Hiawatha seam and the overlying Cottonwood and Blind Canyon seams. Mining is not always feasible in every seam.

The Crandall Canyon property is developed from outcrop, as are almost all coal mines in Utah. Relief is high in the topography of the Wasatch Plateau region; depth of overburden increases rapidly with distance into a mine. Depth to the Hiawatha seam at Crandall Canyon varies with surface topography and ranges roughly between 1,500 and 2,000 ft (450 to 600 m). Thickness is also variable and of the order of 8 ft (2.4 m). Development consists of five nominally 20-ft (6-m) wide main entries separated by 70-ft (21-m) wide pillars driven in an east-west direction. Length of these main entries is about 17,700 ft (4,210 m). Six longwall panels were mined on either side of the main entries from entry ends near a major fault (Joe's Valley

fault) that strikes in a north-south direction. These panels were roughly 780 ft (234 m) wide by 4,700 ft (1,140 m) long on the north side of the main entries and 810 ft (243 m) wide by 7,040 ft (2,112 m) long on the south side. Panels were parallel to the main entries.

FORMULATION OF THE PROBLEM

Finite element analysis is a mature subject and a popular method for solving boundary value problems in the mechanics of solids and other fields as well [e.g., Zienkiewicz, 1977; Bathe, 1982; Oden, 1972; Desai and Abel, 1972; Cook, 1974]. In stress analysis, equations of equilibrium, strain-displacement relationships, and stress-strain laws are requirements met under the constraints of tractions and displacements specified at the boundaries of a region of interest. The method is popular, especially in engineering, because of a relative ease of implementation compared with traditional finite difference methods. The method has important advantages in coping with non-linearity and complex geometry.

Finite element analysis of mining involves computation of stress, strain, and displacement fields induced by excavation. Rock response to an initial application of load is considered elastic. Indeed the elastic material model is perhaps the *de facto* standard model in solid mechanics. However, the range of a purely elastic response is limited by material strength. Beyond the elastic limit, flow and fracture occur, collectively, plastic deformation, i.e., "yielding". Although strictly speaking inelastic deformation is elastic-plastic deformation, "plastic" is used for brevity. Plastic deformation may be time-dependent and various combinations of elastic and plastic deformation are possible, e.g., elastic-viscoplastic deformation allows for time-dependent plasticity beyond the elastic limit.

Generally, excavation takes place in initially stressed ground, so changes in stress are computed. When stress changes are added to the initial stresses, post-excavation stresses are obtained. These stresses may then be used to determine a local factor of safety, the ratio of strength to stress in an element. A safety factor greater than 1.0 indicates a stress state in the range of a purely elastic response to load. A *computed* safety factor less than 1.0 indicates stress beyond the elastic limit, while a safety factor of 1.0 is at the elastic limit where further loading would cause yielding. Unloading from the elastic limit induces an elastic diminution of stress. Safety factors less than 1.0 are physically impossible because yielding prevents stress from exceeding the elastic limit. However, in a purely elastic analysis, computed safety factors may be less than 1.0.

Elastic analyses offer the important advantages of speed and simplicity. Although safety factor distributions based on elastic analysis may differ from elastic-plastic analyses, the differences are not considered important especially in consideration of questions that may arise about the plastic portion of an elastic-plastic material model. Generally, the effect of yielding is to “spread the load” by reducing peak stresses that would otherwise arise while increasing the region of elevated stress.

Mine Geology

A drill hole log of hole DH-7 was used to define the stratigraphic column at Crandall Canyon. This hole is centrally located in the area of interest. Figure 1 shows a color plot of the stratigraphic column used in subsequent analyses. The Hiawatha seam is the thin gray line at the 1,601 ft (480 m) depth. A thickness of 8 ft (3 m) is indicated. Roof and floor are sandstone.

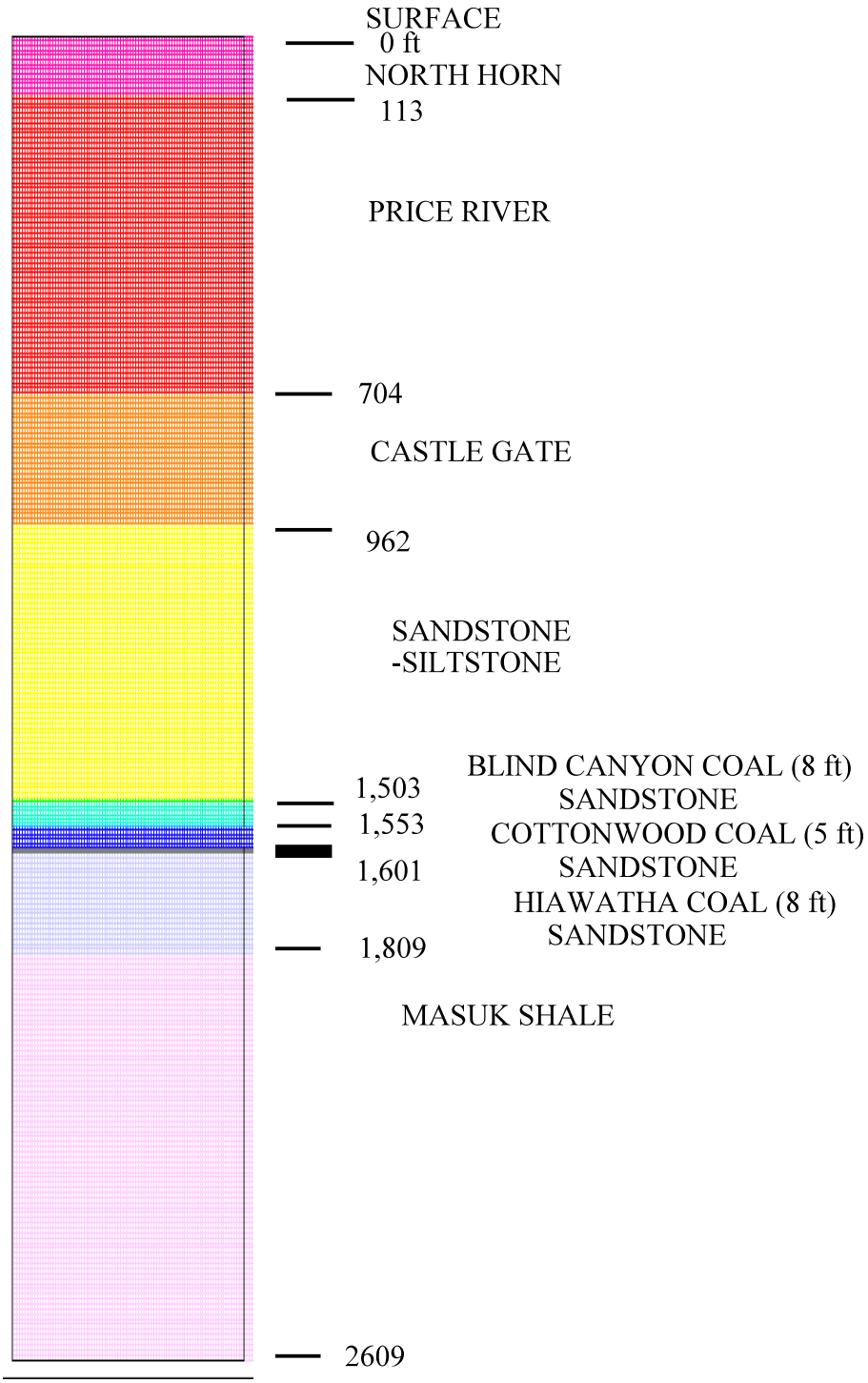

Figure 1. Stratigraphic column, formation names, depths in feet, seam names, and thicknesses (in parentheses in feet). There are 11 layers in the column.

Mine Geometry

The overall region used for analysis is shown in Figure 2 where the colors correspond to the same colors and rock types shown in the stratigraphic column (Figure 1). Details of the main entry geometry are shown in Figure 3. Elements in the mesh shown in Figures 2 and 3 are approximately 10 ft wide and 10 ft high (3.0x3.0 m), except at seam level where element height is 8 ft (2.4 m). Element size is a compromise between interest in detail at seam level and a larger view of panel and barrier pillar mining beyond the main entry development.

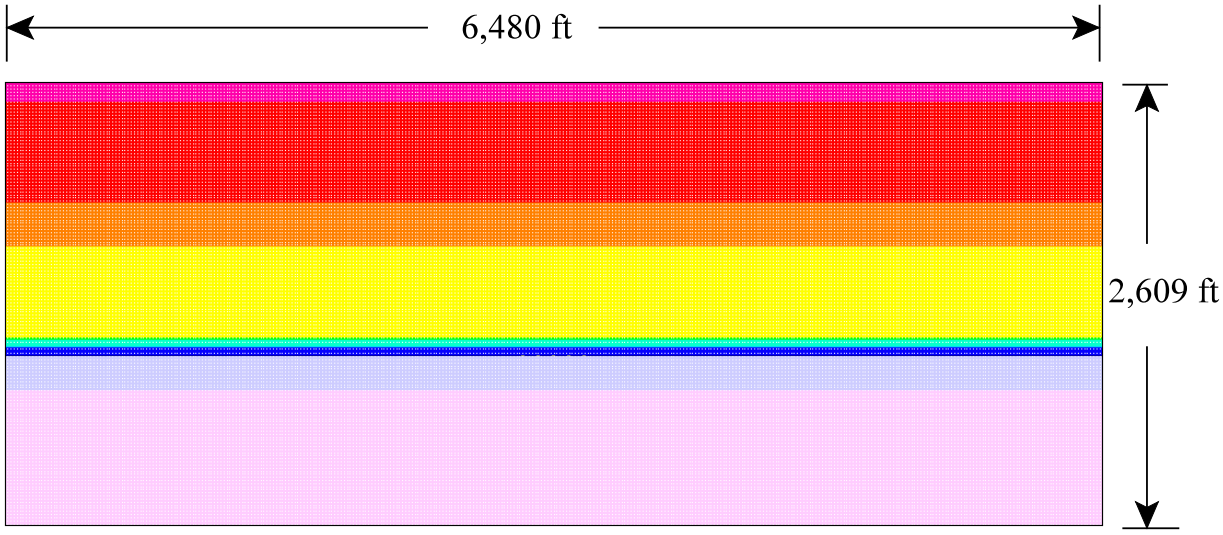

Figure 2. Overall finite element mesh geometry. There are 172,368 elements and 173,283 nodes in the mesh.

The mine geometry changes with development of the main entries and subsequent mining of longwall panels parallel to the mains and on both sides. Barrier pillars 450 ft (135 m) wide are left on both sides of the main entries as shown near seam level in Figure 4. Only 100 ft (30 m) of the future longwall panels are shown in Figure 4. Panels in the analyses are eventually mined 2,600 ft (780 m) on the north and south sides of the main entries. Panels, barrier pillars, main entries and entry pillars account for the 6,480 ft (1,944 m) wide mesh. Cross-cuts are not included in two-dimensional analyses.

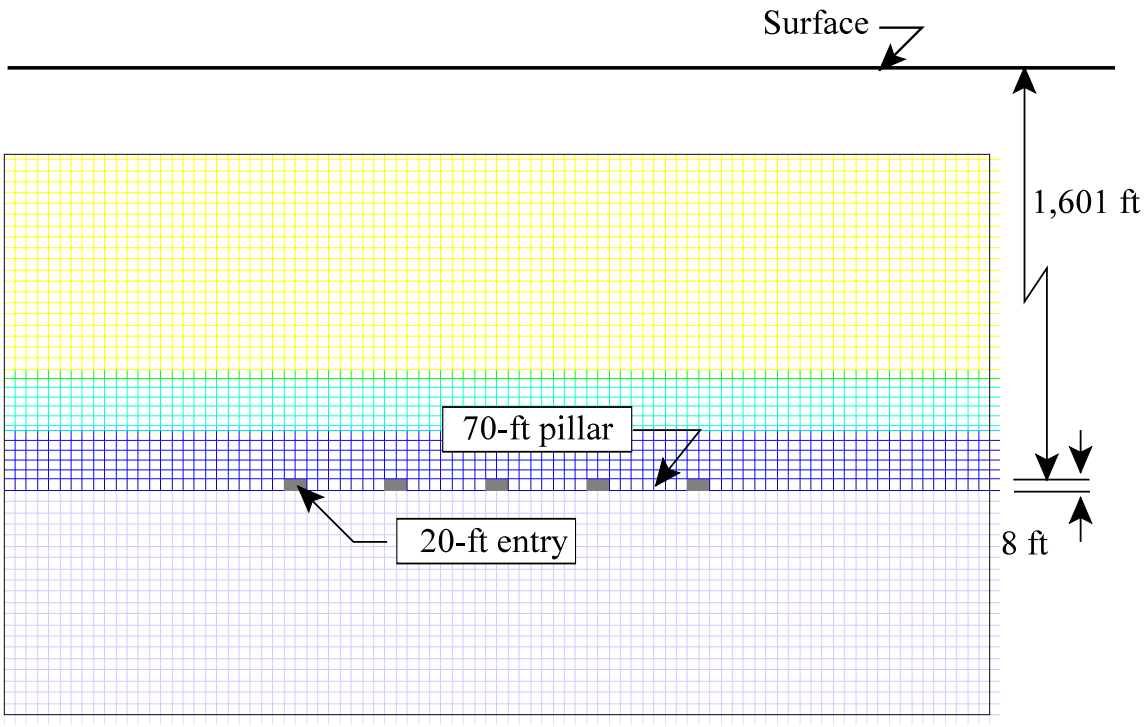

Figure 3. Geometry of the main entries. Coal seam elements are 10x8 ft (3.0x2.4 m).

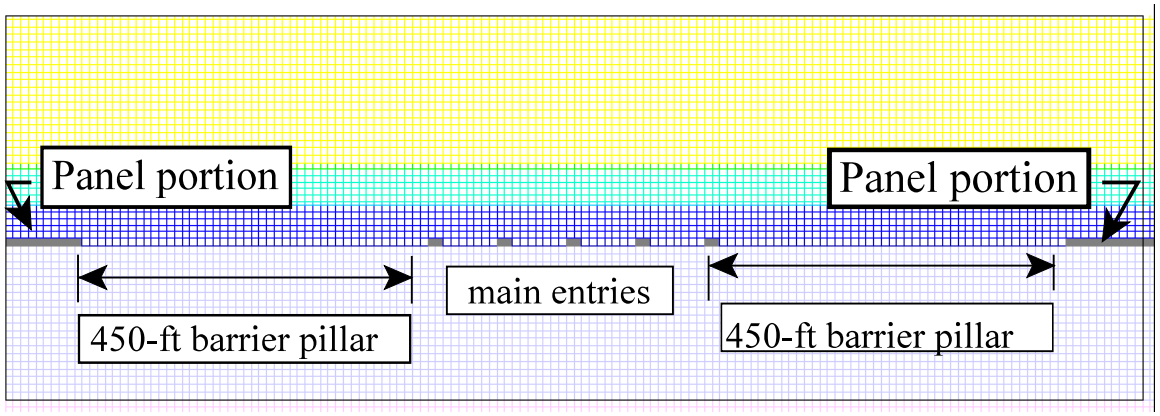

Figure 4. Expanded view at seam level showing main entries, adjacent barrier pillars, and 100 ft (30 m) of future longwall panel excavation.

Premining Stress

The premining stress field is associated with gravity loading only. This simple stress field assumes that the vertical stress before mining is the product of average specific weight of material times depth, or to a reasonable approximation, 1 psi per foot of depth (23 kPa/m of depth). Horizontal stresses are equal in all directions and are computed as one-fourth of the vertical premining stress. Thus, at the top of the Hiawatha seam, the vertical premining stress is 1,601 psi (11.04 MPa) and the horizontal stresses are 400 psi (2.76 MPa). Shear stresses relative to compass coordinates (x=east, y=north, z=up) are nil. Water and gas are considered absent, so these stresses are also the effective stresses before mining. When the depth of cover changes, the premining stresses also change in accordance with the assumed vertical stress gradient and ratio of horizontal to vertical premining stress.

Rock Properties

Rock properties of importance to the present study are the elastic moduli and strengths. The various strata in the geologic column are assumed to be homogeneous and isotropic, so only two independent elastic properties are required, and also only two independent strengths for each material. Young's modulus (E) and Poisson's ratio (ν) are the primary elastic properties and most easily measured. These properties are shown in Table 1 and were adapted from Jones (1994), Rao (1974), and from laboratory tests on core from holes near coal mines in the Book Cliffs field in central Utah. Unconfined compressive and tensile strengths, Co and To, respectively, are the basic strength properties and are also shown in Table 1. Other properties such as shear modulus and shear strength may be computed from the properties given in Table 1 on the basis of isotropy.

Table 1. Rock Properties.

Property / Material	E (10^6 psi)	ν	C_o (10^3 psi)	T_o (10^2 psi)
1. North Horn Formation	2.6	0.26	11.80	7.0
2. Price River Formation	3.2	0.26	9.98	3.8
3. Castle Gate Sandstone	3.0	0.22	9.59	4.3
4. Sand+Siltstone	3.1	0.24	13.50	11.9
5. Blind Canyon Coal	0.43	0.12	4.13	2.8
6. Roof/Floor Siltstone	2.8	0.23	12.18	12.9
7. Cottonwood Coal	0.43	0.12	4.13	2.8
8. Roof Sandstone	3.4	0.26	14.50	10.9
9. Hiawatha Coal	0.43	0.12	4.13	2.8
10. Floor Sandstone	3.4	0.26	11.72	11.7
11. Masuk Shale	2.2	0.35	10.30	0.60

Compressive strength of rock is generally dependent on confining pressure as shown in laboratory tests. The well-known Mohr-Coulomb strength criterion is one way of expressing confining pressure dependency. This criterion may be expressed in terms of the major and minor principal stress at failure in the form

$$(1/2)(\sigma_1 - \sigma_3) = (1/2)(\sigma_1 + \sigma_3)\sin(\phi) + (c)\cos(\phi) \qquad (1)$$

where $\sigma_1, \sigma_3, c, \text{and } \phi$ are the major principal stress, minor principal stress, cohesion and angle of internal friction, respectively, and compression is positive. The left side of (1) is the maximum shear stress, while the sum of the principal stresses on the right side is a mean normal stress in the plane of the major and minor principal stresses. Cohesion and angle of internal friction may be expressed in terms of the unconfined compressive and tensile strengths. Thus,

$$\sin(\phi) = \frac{C_o - T_o}{C_o + T_o}, \quad c = (\frac{1}{2})\sqrt{C_o T_o} \tag{2}$$

An alternative form of (1) that shows the direct dependency of compressive strength on confining pressure is

$$C_p = C_o + (\frac{C_o}{T_o})p \tag{3}$$

where C_p and p are compressive strength under confining pressure and confining pressure, respectively. Equation (3) has applicability to pillar strength because often a pillar is much wider than it is high and has a core confined by horizontal stress. The ratio of unconfined compressive strength to tensile strength in (3) is often 10 or greater and thus multiplies the confining pressure effect by an order of magnitude or more.

Often the increase of compressive strength with confining pressure is non-linear and moreover the intermediate principal stress may influence strength. A criterion that handles both possibilities is a non-linear form of the well-known Drucker-Prager criterion that may be expressed as

$$J_2^{N/2} = AI_1 + B \tag{4}$$

where compression is positive and $J_2, I_1, N, A, \text{and } B$ are second invariant of deviatoric stress, first invariant of stress, an exponent, and material properties, respectively. The variable $\sqrt{J_2}$ is a measure of shear stress intensity, while I_1 is a measure of the mean normal stress that includes the three principal stresses. The last two, A and B, may be expressed in terms of the unconfined compressive and tensile strengths, while the exponent (N) is decided upon by test data. A value

of 1 reduces (4) to the original Drucker-Prager criterion. A value of 2 allows for non-linearity and more realistic fits to test data. A value $N = 2$ is used in this study. The maximum value of $J_2^{1/2}$ for the given mean normal stress ($I_1 / 3$) can be extracted from (4). The ratio of this maximum value to the actual value is a factor of safety for the considered point. Thus, an element factor of safety $fs = J_2^{1/2}$ (strength) / $J_2^{1/2}$ (stress). This ratio has an analogy to the ratio of shear strength to shear stress. Uniaxial compression and tension are special cases included in this definition of element safety factor. Other definitions are certainly possible, but the one described here is embedded in UT2 and serves the important purpose of indicating the possibility of stress exceeding strength and thus the possibility of yielding.

Mining Sequence

The mining sequence involves several stages: (1) excavation of the main entries, (2) excavation of panels on either side of the main entries, (3) entry excavation in the north barrier pillar, (4) entry excavation in the south barrier pillar. Main entries are excavated in strata initially stressed under gravity loading alone. Stress changes induced by mining entries are added to the initial stresses to obtain the final stresses at the end of main entry excavation. These final stresses are the initial stresses for the next stage of excavation (panel mining) and so on.

Boundary Conditions

Displacements normal to the sides and bottom of the mesh shown in Figure 2 are not allowed, that is, they are fixed at zero. The top surface of the mesh is free to move as mining dictates. Initial conditions are boundary conditions in time. These are the stresses at the start of each excavation stage.

There is a possibility that computed seam closure, the relative displacement between roof and floor, may exceed mining height. This event is physically impossible and thus must be prohibited by appropriate boundary conditions. Because the bottom of the mesh is fixed in the vertical direction, floor heave is somewhat restricted relative to a mesh of greater vertical extent. Roof sag is not restricted, so specification of roof sag in an amount that prevents overlap of floor heave is a reasonable physical constraint to impose as an internal boundary condition. Where overlap of roof and floor does not occur, no constraint is necessary.

FINITE ELEMENT ANALYSIS

The main results of an analysis are stress, strain and displacements induced by mining. Visualization of information derived from these basic results assists in understanding strata mechanics associated with mining and in assessment of overall safety of a particular mining plan. Color contours of element safety factors are especially helpful. In two-dimensional analyses, variables such as widths of entries, pillars, panels and barriers may be changed at will as may other input data including stratigraphy and rock properties. The list of parameters is long; a design parameter study on the computer could be lengthy, indeed. However, in a case study, the input is fixed and thus computation time is greatly reduced. When the stratigraphic column extends to the surface, subsidence may be extracted from displacement output. If the actual subsidence profile is known, a match between finite element model output and mine measurements may be used to constrain the model in a reasonable manner.

Main Entry Mining

Figure 5 shows before and after views of main entry mining. The "before" view is just the mesh shown in Figure 3, but to the same scale as the "after" view that shows the distribution of the element safety factors according to the color scale in the figure. The three yellow bands are coal seams and show almost a uniform safety factor of 2.7 away from the main entries. Pillars between the entries and ribs of the outside entries show a slightly lower safety factor of 2.2. Roofs and floors show much higher safety factors (greater than 4.5) because of the greater strength of roof and floor strata. Pillar safety factors are with respect to compressive stress as inspection of the stress output file shows. A safety factor of 2 to 4 in compression is suggested in the literature [Obert and Duvall 1967], so the main entry system is considered safe.

Stress concentration in great detail is *not* obtained in this analysis stage because of the relatively coarse mesh that uses 10x8 ft (3.0x2.4m) coal seam elements about an entry 20 ft (6 m) wide by 8 ft (2.4 m) high. In fact, element stresses are average stresses over the area enclosed by an element. Stresses in a pillar rib element are average stresses over the 10 ft (3 m) distance into the rib and over the full mining height of 8 ft (2.4 m). A highly refined mesh would reveal details about an entry and perhaps compressive stress concentrations enough to cause yielding at entry ribs and tensile stress concentrations possibly high enough to cause roof and floor failure. Such effects would necessarily be localized within about a half-element thickness (5 ft, 1.5 m) because no failure in ribs, roof, and floor is indicated in elements adjacent to the main entries in Figure 5. Figure 6 shows the distribution of vertical and horizontal stress across the main entries and pillars. The U-shape pattern is typical of vertical stress after mining. The horizontal stress increases from zero at the ribs with distance into the rib rather rapidly because of element size.

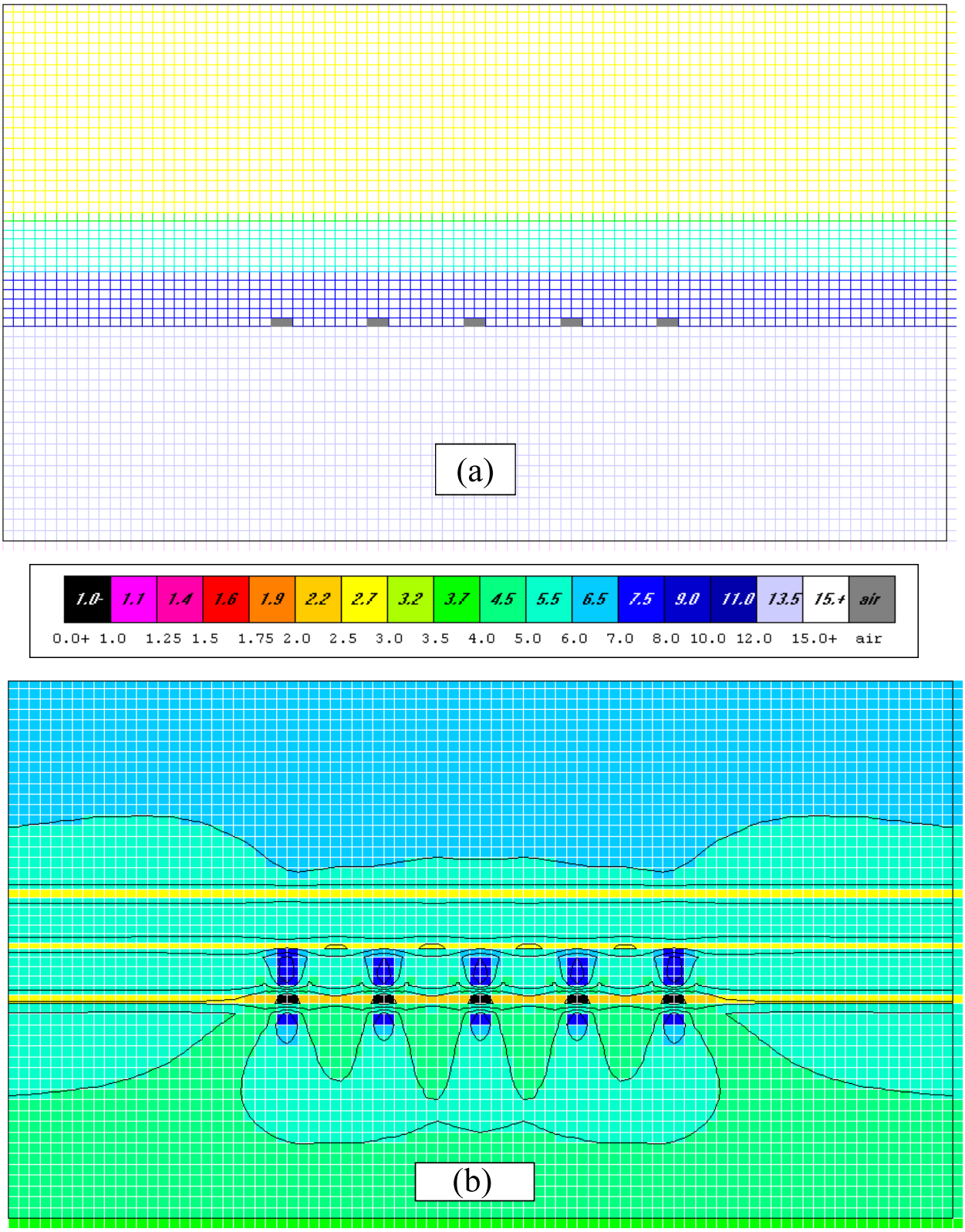

Figure 5. Element safety factor distribution. (a) before mining main entries, (b) after mining.

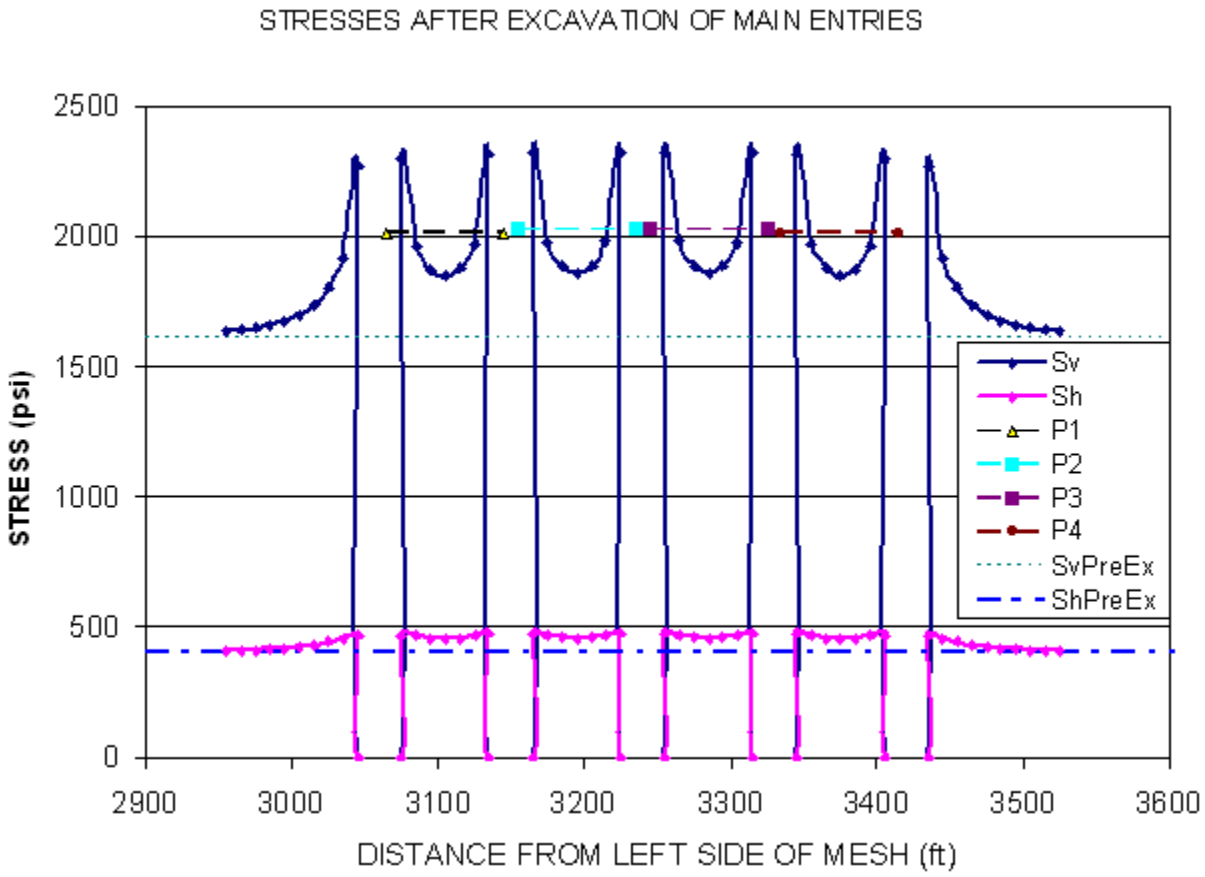

Figure 6. Stress distribution across the main entries and pillars after excavation. Sv=vertical stress, Sh=horizontal stress. Dashed lines are premining values.

The average vertical stress in each pillar in Figure 6 is shown by the horizontal lines labeled P1, P2, P3, and P4. These values are obtained from the finite element analysis and have an overall average of 2,021 psi (13.9 MPa). A tributary area or extraction ratio calculation gives a slightly higher average of 2,057 psi (14.2 MPa) because of the assumption of an infinitely long row of entries and pillars. The average vertical pillar stress is well below the unconfined compressive strength of coal. In fact, the ratio of strength to average vertical stress is a safety factor of sorts with a value of 2.0. Because the vertical stress varies across a pillar and horizontal stress increases confinement with distance into a pillar, the local element safety factor varies

through a pillar. This variation is shown in Figure 7 where data are from finite element results and the local factor of safety (*fs*) is based on the formulation used in UT2. Also shown in Figure 7 is a normalized vertical stress obtained by dividing the post-mining vertical stress (Sv) by the premining vertical stress (So), in essence, a stress concentration factor for vertical stress. The local safety factor is least at the pillar ribs where confinement is nil and vertical stress is high and greatest at the core of the pillar where confinement is high and vertical stress is less concentrated than at the rib. The close agreement between the tributary area calculation of vertical pillar stress after mining and the finite element results provides a check on the finite element analysis.

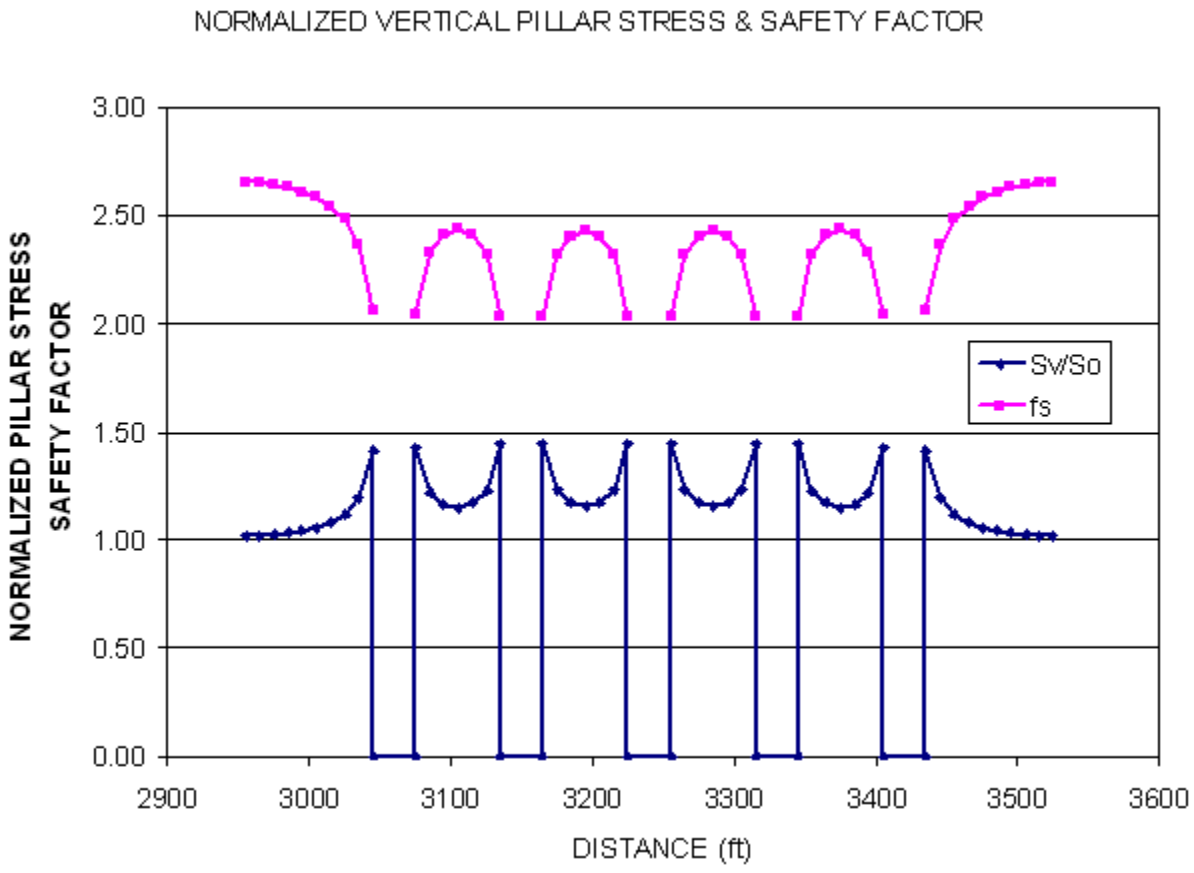

Figure 7. Pillar safety factor distribution from UT2 data and normalized vertical stress across the main entries and pillars.

Longwall Panel Mining

Six longwall panels were mined on the north and south sides of the main entries that were excavated in an east-west direction. For the most part, two panel entries were used for development. The chain pillars of the panel entries undoubtedly are lost as a panel is mined and are not considered in analysis of panel excavation effects on the main entries. Six panels approximately 780 ft to 810 ft (234 m to 243 m) wide were excavated on each side of the main entries. Barrier pillars approximately 450 ft (135 m) wide separate the nearest of these panels from the main entries. In the second stage of finite element analysis, panel mining extends 2,600 ft (780 m) on each side of the barrier pillars. The geometry of this stage of analysis is shown in Figures 2, 3, and 4.

Node Displacements and Subsidence. The first analysis of panel mining was only partially successful. While the solution process proceeded monotonically and convergence was excellent, roof and floor displacements over the central portions of the excavated panels indicated seam closure greater than seam thickness, a physical impossibility. A correction was applied in the second analysis that prevented excess seam closure. In this analysis, seam closure was set in a way that allowed maximum surface subsidence over the panel centers to approximate observed surface subsidence while preventing roof-floor overlap. Thus, seam level roof sag was restricted over the horizontal length of 1,300 ft (390 m) from panel centers (mesh sides). No restrictions on floor heave were imposed. Subsidence profiles across panels 13 through 17 on the south side of the main entries that were plotted for the years 1999 through 2002 indicated formation of a flat subsidence trough with about 5 ft (1.5 m) of surface subsidence.

Figure 8a shows displacements in the form of a deformed mesh after a second attempt at panel mining. The displacement scale is exaggerated relative to the distance scale in order to visualize the overall displacement pattern. Maximum displacement of 63 inches or about 5 ft (160 cm or about 1.5 m) occurs at the mesh sides, that is, over the centers of panel mining. Interestingly, 18 inches (46 cm) of subsidence occurs over the center of the main entries. Floor heave (upward displacement) is also maximum at the mesh sides but diminishes with distance to the main entries. At 130 ft (39 m) from the outside barrier pillar ribs, floor heave diminishes to zero. With further distance from the mesh sides towards the mesh center and center of the main entries, floor displacement is downwards indicating that the barrier pillars and entry pillars depress the floor under the weight transferred from panel mining. Figure 8b is a close up view of the deformed mesh about the main entries and only hints at entry roof sag and floor rise. The rough agreement between maximum subsidence obtained from finite element analysis and that observed in actual subsidence profiles, although indirectly imposed through seam closure, suggests the finite element model of panel mining is reasonable.

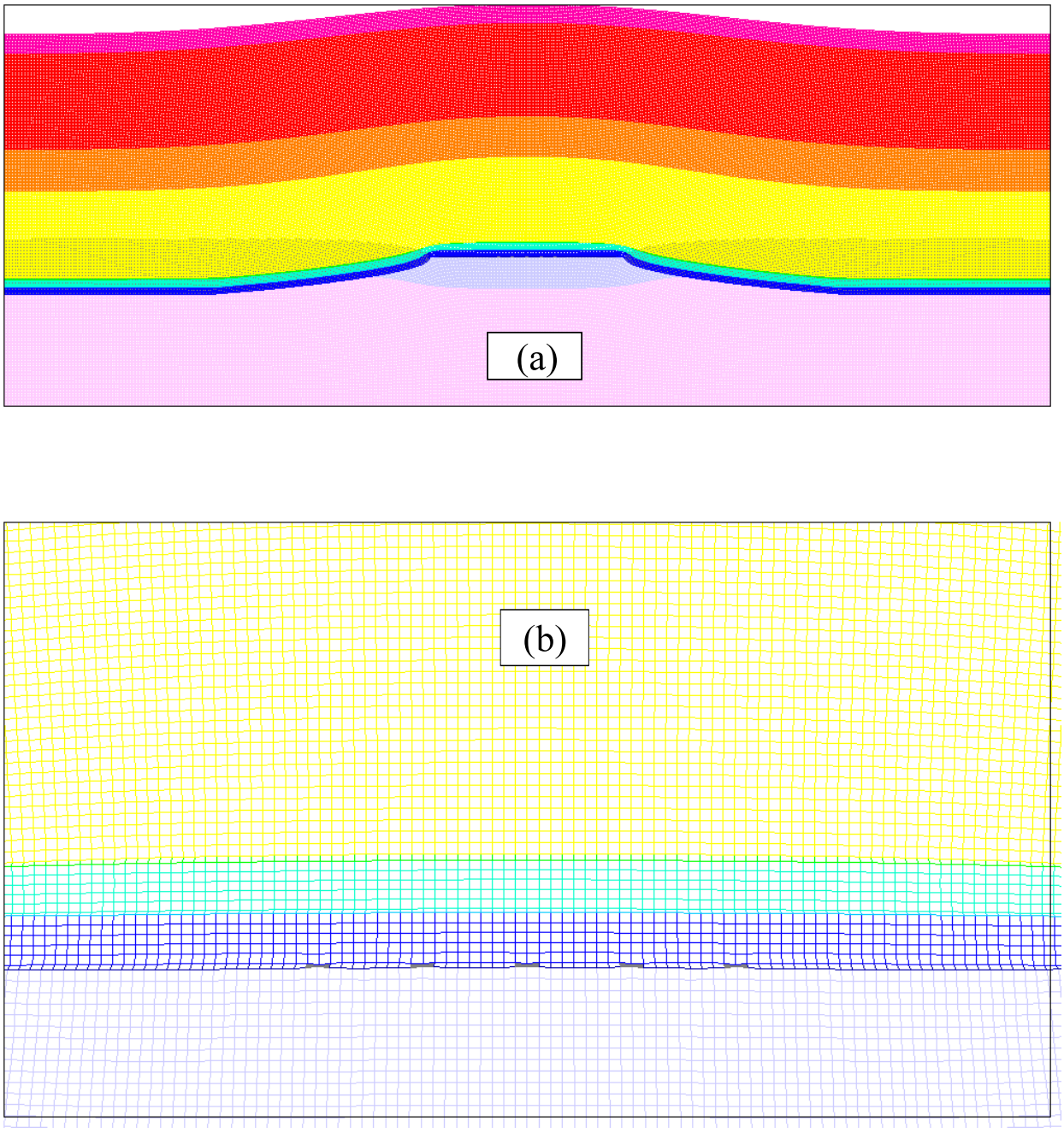

Figure 8. Displacements after panel and entry mining. (a) overall, (b) entries.

Element Safety Factor Distributions. Element safety factor distributions reveal at a glance areas that have reached the elastic limit and are therefore subject to yielding and areas well below the elastic limit and of much less concern. Safety and stability of an entry surrounded by an extensive zone of yielding would surely be threatened. A pillar with all elements stressed beyond the elastic limit would also be of great concern. Absence of extensive zones of yielding would be reassuring.

Figure 9 shows the overall distribution of element safety factors in two ways, one without contours that supplement the color coding and one with contours. The seemingly faded color is a result of the plot density that brings white element borders into close proximity and allows only a tiny area for coloring. The jumps in contours occur across strata interfaces where discontinuities in material properties occur. Disruption of contours occurs at seam level across portions of the seam that have been excavated (panels and entries). Symmetry of the contour pattern is apparent and as the pattern should be. The dark (black) regions of yielding are extensive. Near the surface above the main entries strata flexure leads to tensile failure. Much of the roof and floor yield is also tensile.

An expanded half-mesh view is shown in Figure 10 where the yield zones are more clearly seen. Strata flexure in tension and failure is indicated near seam level in the roof outside the barrier pillar rib. Floor failure below is also evident in Figure 10. Interestingly, yielding is small in the immediate sandstone floor, but is extensive in the Masuk shale below.

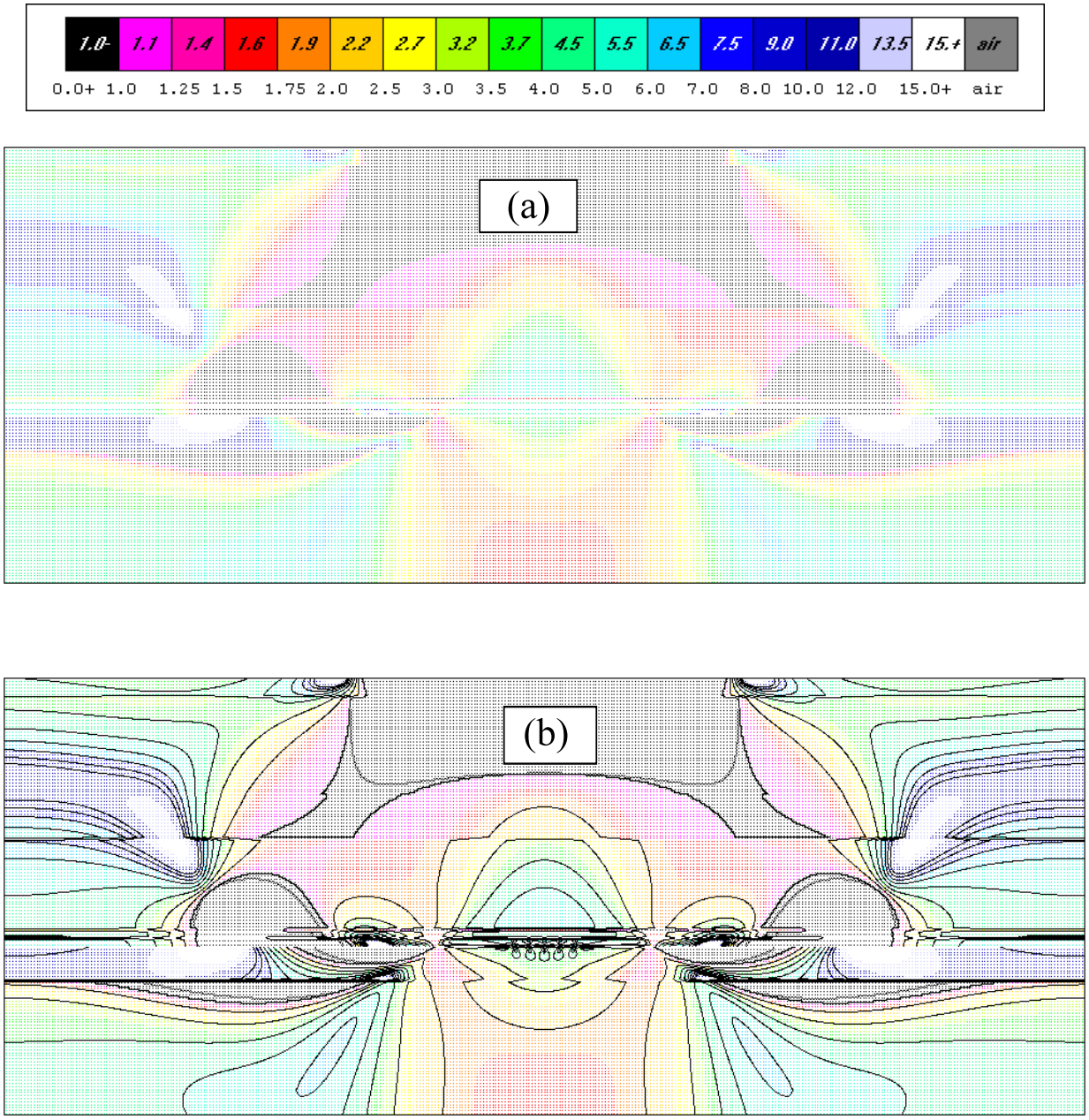

Figure 9. Whole mesh element safety factor distributions. (a) without line contours, (b) with.

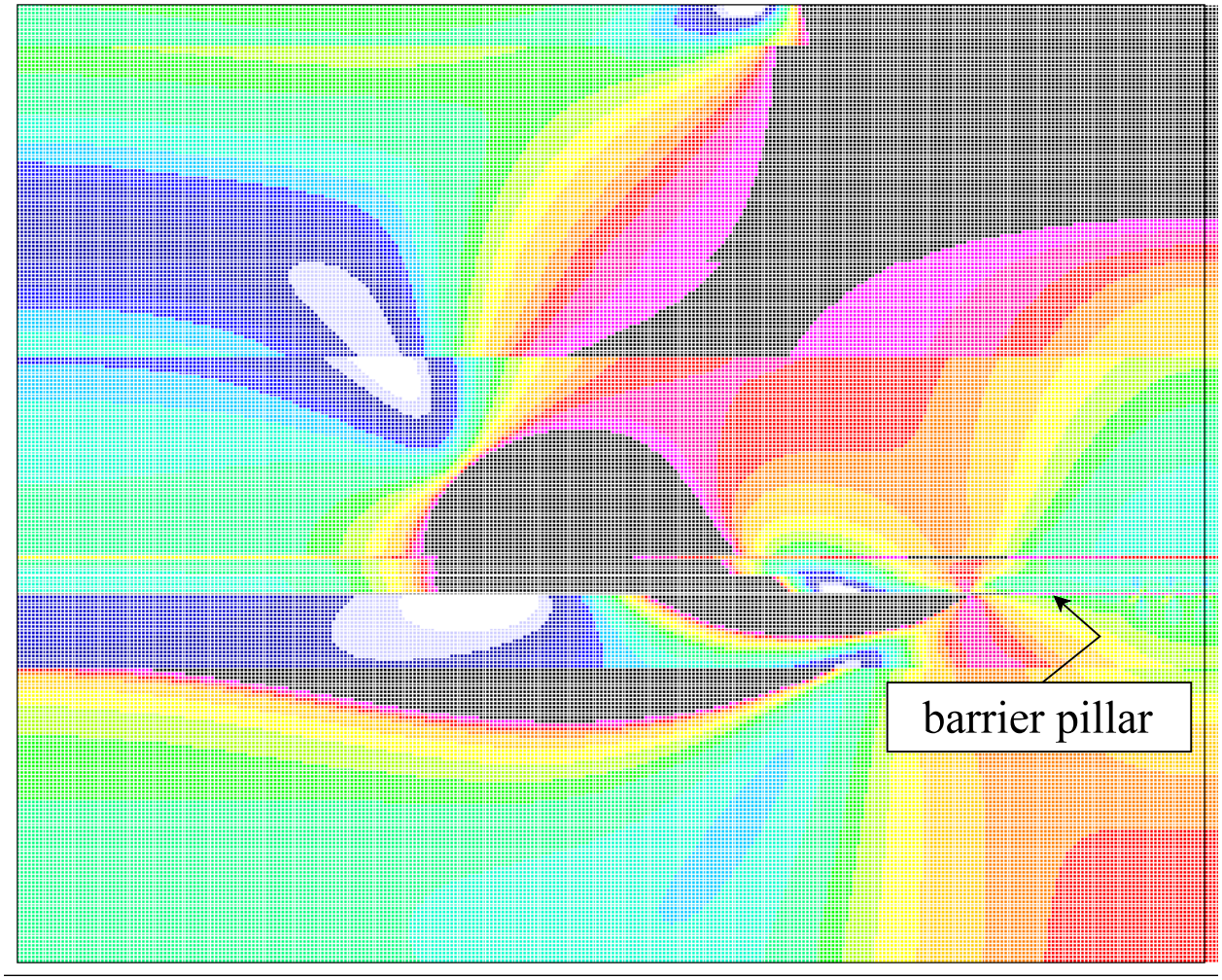

Figure 10. A half-mesh view of element safety factors showing dark (black) zones of yielding mainly in horizontal tension associated with strata flexure.

Yielding under high compressive stress penetrates the barrier pillar from the panel side a distance of 110 ft (33 m). Thus, about 25% of the barrier yields after panel excavation. This penetration is accompanied graphically by large horizontal excursions of the safety factor contour lines in Figure 11 which shows details of the element safety factor distribution in the vicinity of a barrier pillar. Half of the main entries are included in Figure 11. The remainder of the barrier pillar while not yielding is highly stressed with element safety factors no greater than 1.34. Yielding in the two overlying coal seams is evident in a region above the barrier pillar.

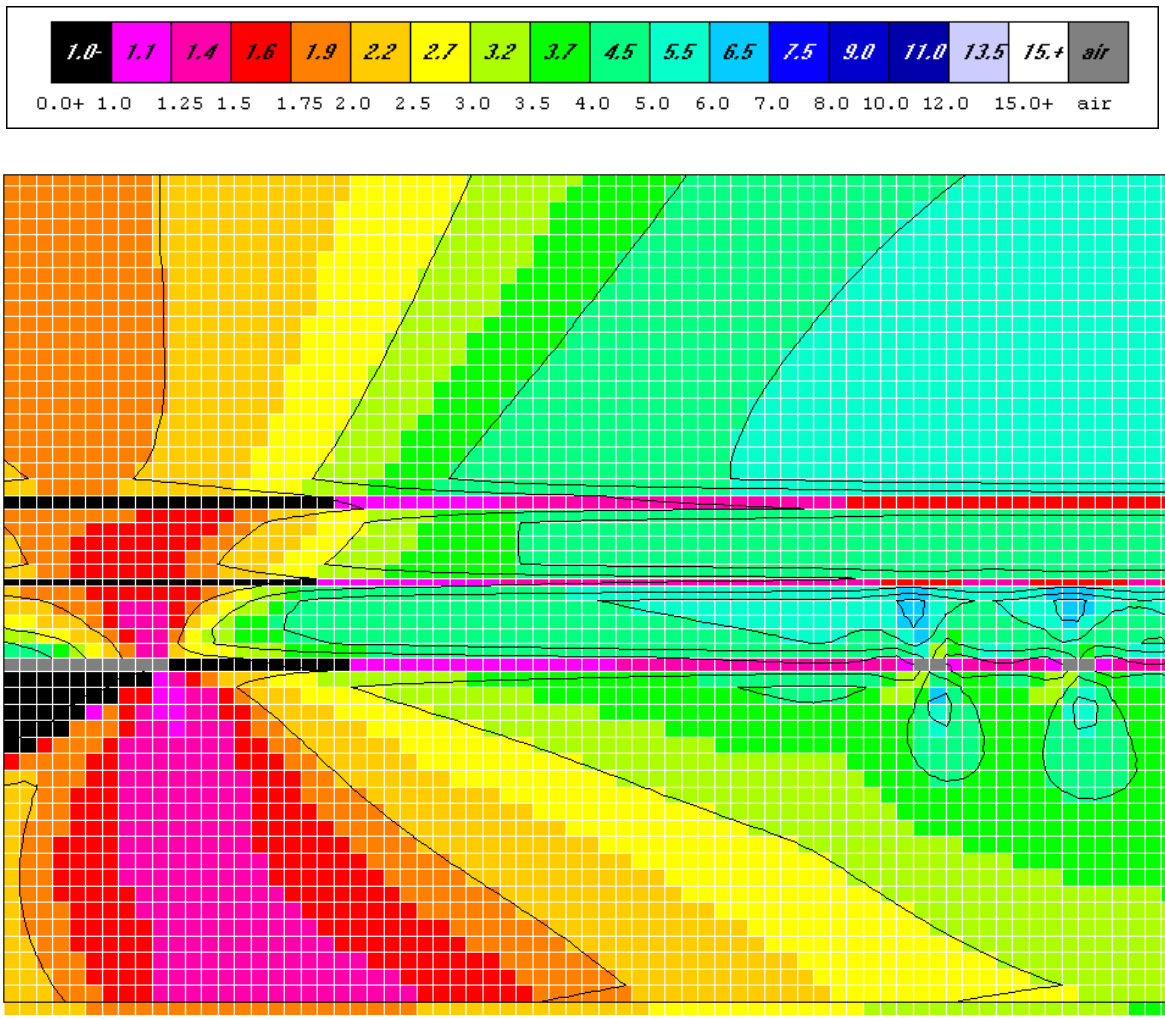

Figure 11. Element safety factors about a barrier pillar after panel mining.

Details of the element safety factor distribution about the main entries is shown in Figure 12. The pink and red zones indicate relatively low safety factors. The highest safety factor in the main entry pillars is 1.34, the same peak value in the barrier pillars on either side of the main entries. Thus, all pillar element safety factors are less than the minimum of 2 recommended by Obert and Duvall (1967). Roof and floor safety factors are in the 4 to 5 range. Although mesh refinement would lead to lower safety factors at the roof and floor of an entry, there appears to be no significant threat to roof and floor safety at this stage of mining.

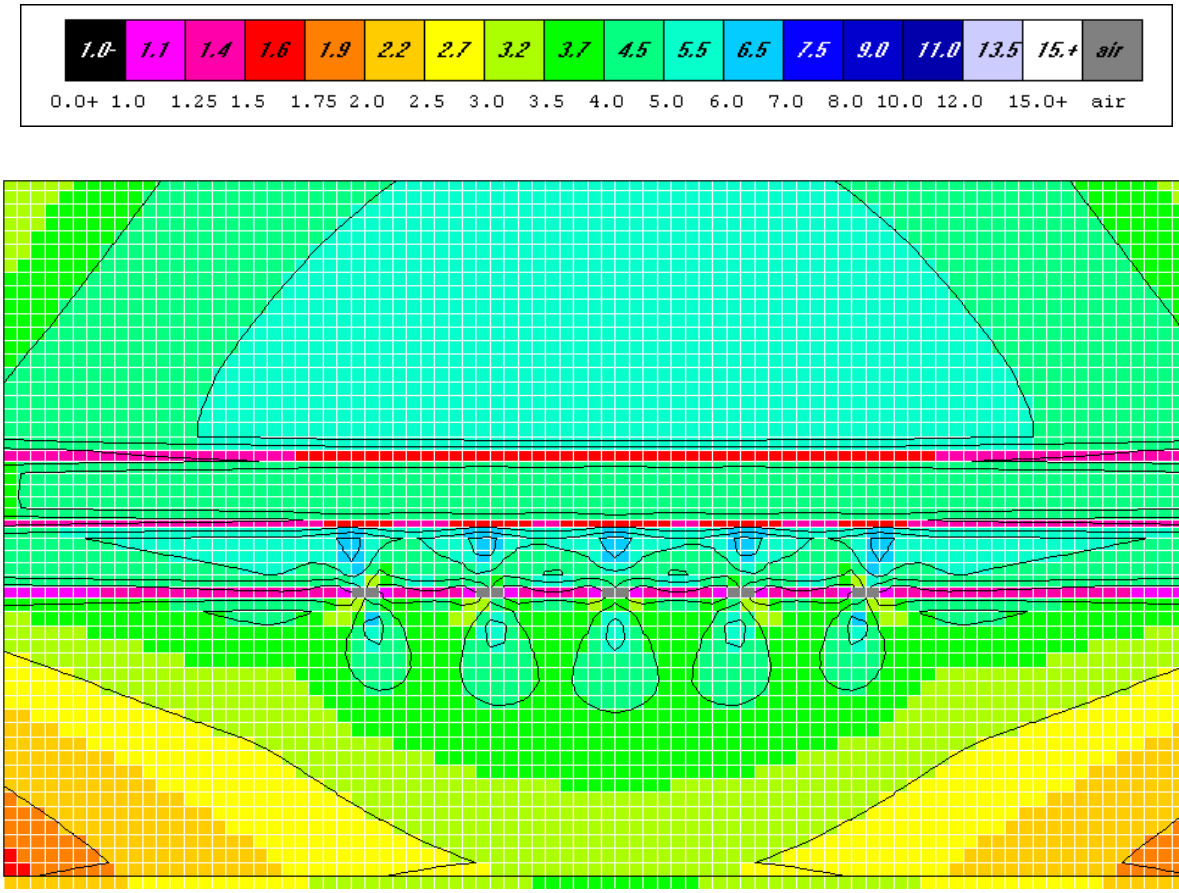

Figure 12. Distribution of element safety factors about the main entries after panel mining.

Barrier Pillar Entry Mining

Barrier pillar entry mining in the analysis consists of four entries 20 ft (6 m) wide separated by pillars 60 ft (18 m) wide. Two sets of such entries were mined, one on the north side and one on the south side of the original main entries. The north side barrier pillar entries were separated from the north side longwall panels by a pillar 140 ft (42 m) wide and from the main entries by a pillar 50 ft (15 m) wide. The south side barrier pillar entries were separated from the south side longwall panels by a 120 ft (36 m) wide pillar and from the original main entries by a 70 ft (21 m) pillar. These dimensions were estimated using the distance function in a drawing of the mine geometry. Without doubt, the as-mined dimensions differ from these

nominal dimensions. Provided such dimensional differences are small, finite element results should differ only slightly as well and not affect inferences from analysis results concerning overall safety of the mining plan.

North Barrier Pillar Mining. The third stage of analysis follows the first and second stages of main entry development and panel mining. This stage involves further entry and pillar development in the north barrier pillar. Mining geometry is illustrated in Figure 13 and shows four additional entries and associated pillars. Only 100 ft (30 m) of the 2,600 ft (780 m) of prior panel mining is shown in Figure 13. Mining height is 8 ft (2.4 m) as before.

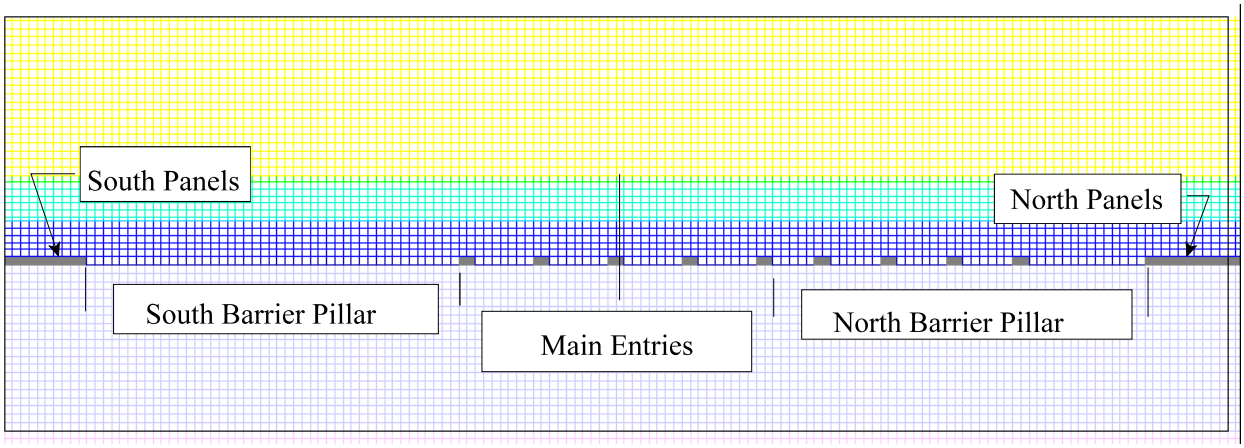

Figure 13. North barrier pillar entry geometry.

The distribution of element safety factors after entry development in the north barrier pillar is shown in Figure 14. Most elements in the north side barrier pillar are now at yield. Rib elements in pillars adjacent to the original main entries are also at yield. The outside entry of the original main entries shows ribs yielding in the pillar between it and the new north side barrier pillar entry. The south outside entry ribs shows yielding extending 10 ft (3 m) into the ribs. The highest safety factor in any pillar element in Figure 14 is 1.2.

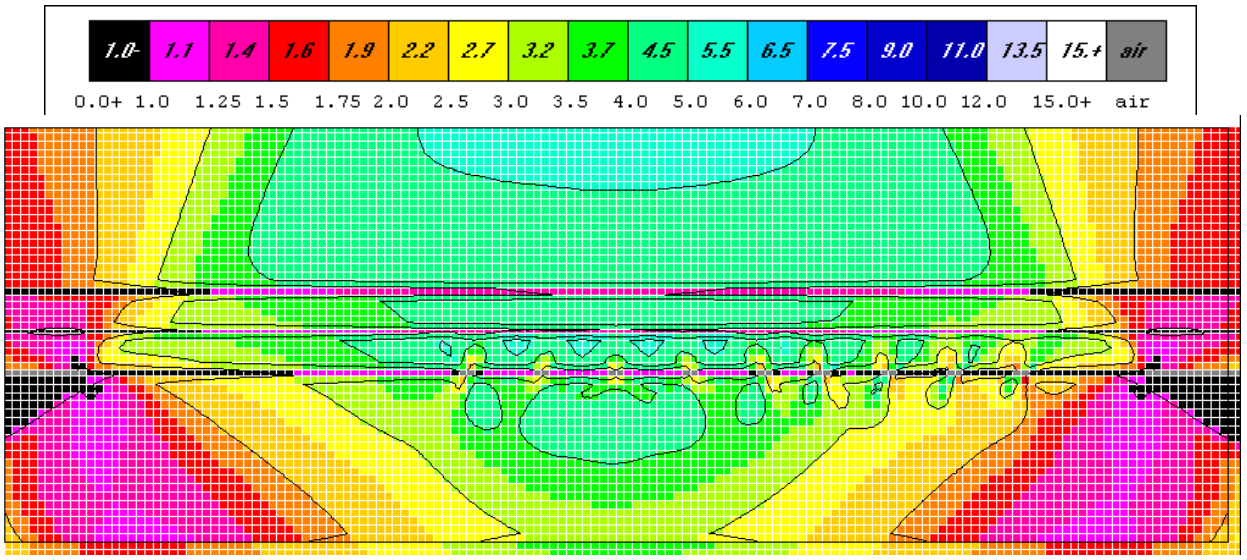

Figure 14. Element safety distribution after entry development in the north barrier pillar.

South Barrier Pillar Mining. The fourth and last stage of analysis is entry development in the south barrier pillar and follows entry development in the north barrier pillar. Mining geometry is illustrated in Figure 15 and shows four additional entries and associated pillars in the south barrier pillar. Only 100 ft (30 m) of prior panel mining is shown in Figure 15. Mining height is 8 ft (2.4 m). Entry and pillar widths in the south barrier pillar development are 20 ft (6 m) and 60 ft (18 m), respectively. Four additional entries are developed in the south barrier pillar.

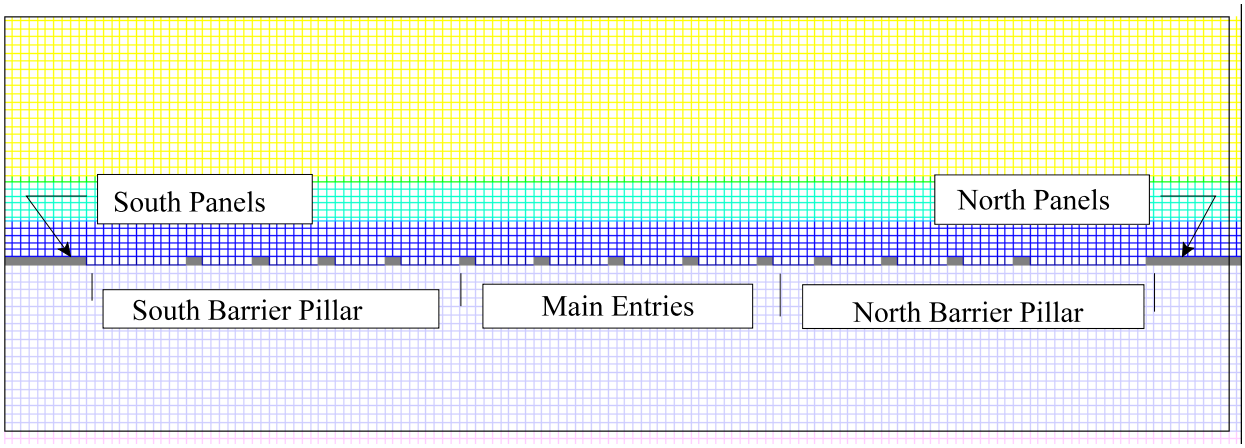

Figure 15. South barrier pillar mining geometry.

The distribution of element safety factors after entry development in the south barrier pillar is shown in Figure 16. Almost all elements in the south side barrier pillar are now at yield. Indeed all pillar elements across the mining horizon are close to yield. Peak vertical stress in the barrier pillars exceeds 38,400 psi (264.8 MPa), over 9 times the unconfined compressive strength of the coal. Horizontal stress exceeds 7,300 psi (50.3 MPa). Even so this high confining pressure is insufficient to prevent yielding. The lowest vertical pillar stress is about 6,000 psi (41.4 MPa), almost half again greater than the unconfined compressive strength of the coal; the lowest horizontal pillar stress is about 1,500 psi (10.3 MPa). Any release of horizontal confinement would likely result in rapid destruction of pillars. Additionally, entries nearest to the mined panels are showing reduced roof and floor safety factors. Yield zones extend to depth in the floor. Overlying coal seams are also yielding or are very close to yielding over portions of the barrier pillars, as seen in Figure 16.

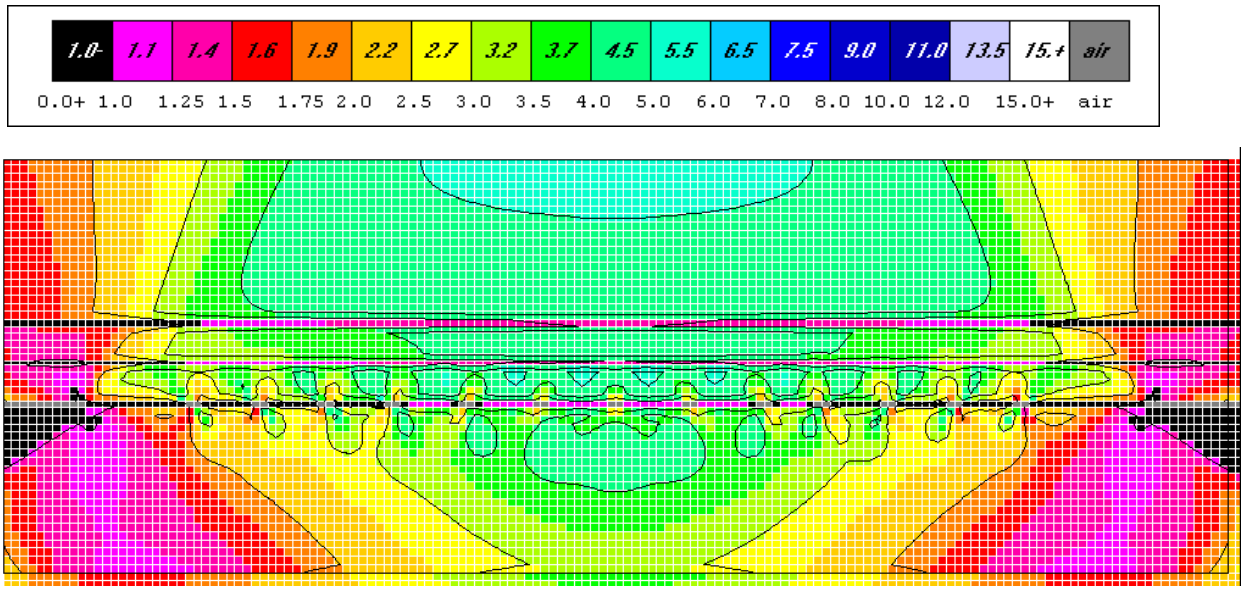

Figure 16. Element safety distribution after entry development in the south barrier pillar.

Figure 17 shows the distribution of element safety factors about the original main entries after entry mining in the north and south barrier pillars. Roof and floor element safety factors have decreased significantly from the original values obtained during development prior to longwall panel mining and range between 2 and 4, as seen in the color code. Roof and floor element safety factors about the new entries mined in the barrier pillars are lower, roughly in the range of 2 to 4 in Figure 17.

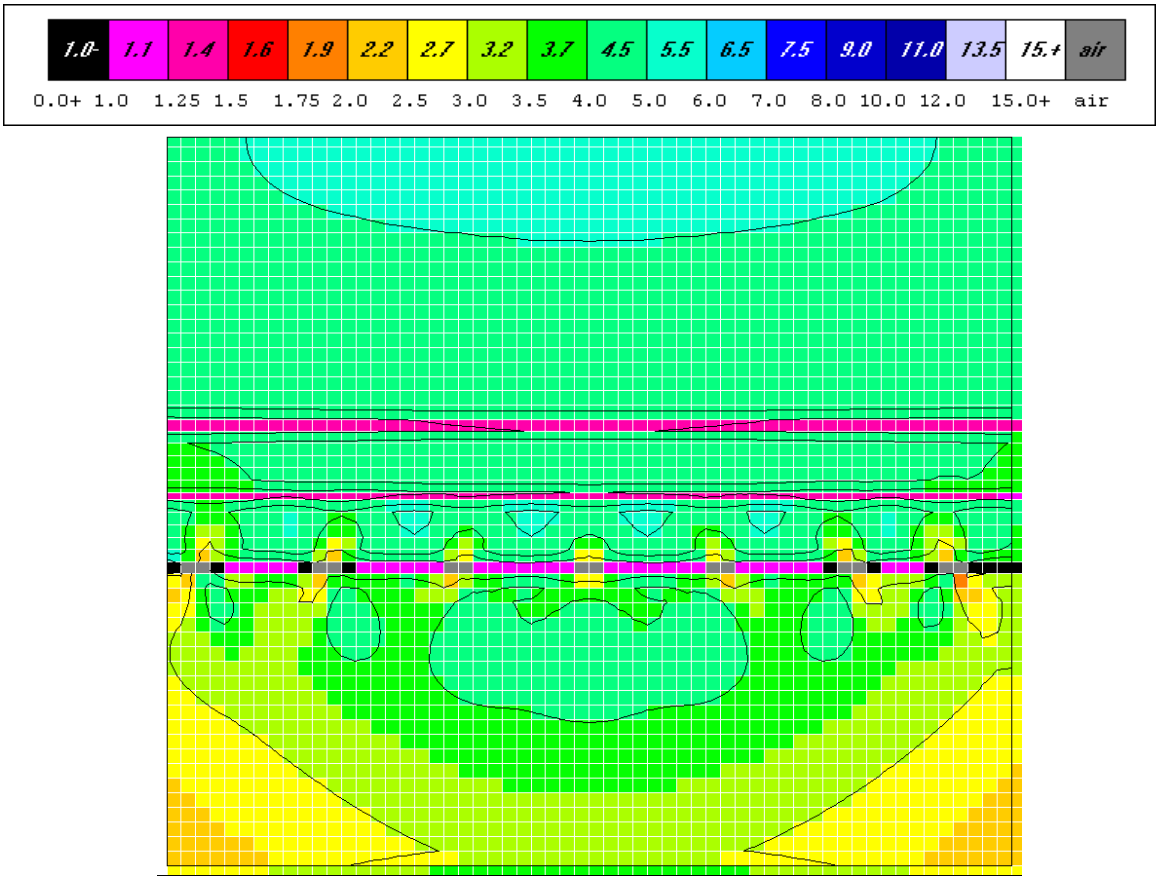

Figure 17. Distribution of element safety factors about the original main entries after development in the north and south barrier pillars.

The distribution of horizontal and vertical element stresses after main entry development, panel mining, and entry development in the north and south barrier pillars is shown in Figure 18 where gaps are entry elements. The very high vertical stresses on the ribs of the barrier pillars

adjacent to the panels mined north and south of the barrier pillars is striking. Although these extreme peaks in vertical stress diminish rapidly across the pillars, they remain well above the unconfined compressive strength of the coal, also shown in Figure 18. Recall the analysis is elastic. If yielding were allowed as in an elastic-plastic analysis, these peaks would diminish and the extent of yielding would likely spread across regions of the pillars that have not yielded according to the elastic results. Horizontal confinement in rib elements at the ribs of the barrier pillars, where the vertical stress is high, is because of averaging over the width of rib elements. The actual horizontal stress at the rib must be zero. The high analysis value is associated with mesh refinement and the use of a 10 ft (3 m) wide element. A lower horizontal stress would enhance the spread of pillar yielding. Again, purely elastic behavior leads to an underestimate of the extent of yielding that is indicated by elements with a safety factor less than one.

A tributary area calculation of the average pillar stress across the entire seam is also shown in Figure 18 as is the finite element analysis result. These two values agree within one percent and lend credence to the analysis. In essence, the calculation shows that the requirement for equilibrium of stress in the vertical direction is satisfied in the course of four stages of mining. Any analysis result, regardless of method, should meet this requirement.

Figure 19 shows the distribution of element safety factors at seam level. Safety factors less than one are a consequence of a purely elastic calculation. Safety factors less than one indicate a potential for shedding stress to adjacent elements.

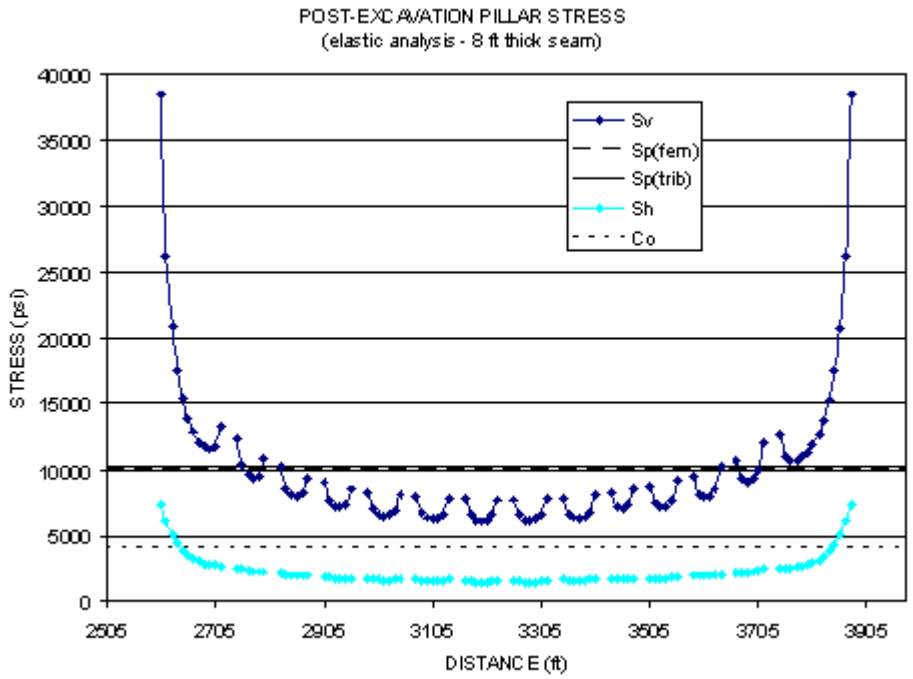

Figure 18. Post-excavation pillar stress distribution. Sv=premining vertical stress. Sp=average pillar stress, fem=finite element method, trib=tributary area, Co=unconfined compressive strength.

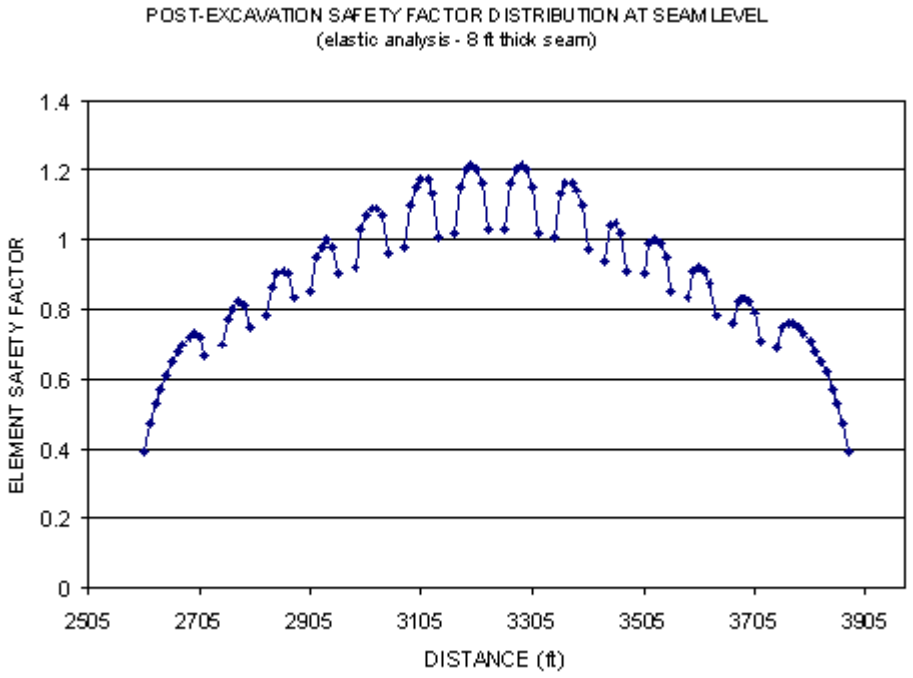

Figure 19. Post-excavation element safety factor distribution.

DISCUSSION

Several questions that often arise about finite element analysis involve input data, two-dimensional analysis, and interpretation of output results. A brief discussion of these questions may not alleviate concerns, but does allow for some explanation and expression of opinion.

The first issue here is the proverbial one about quality of input data and consequences for output results. In fact, this question is present in all engineering analysis and is not unique to the finite element method or other computer-based models for stress analysis or for the analysis of business plans and so forth. Generally, the problem of mine excavation using UT2 is a well-posed mathematical problem in solid mechanics, so small variations in input data lead to only small variations in output. However, if there are errors in input, then the output will also be erroneous. For this reason, checks on results are important when available. An extraction ratio calculation after main entry excavation indicates reliable output at this stage of analysis. Subsidence results in agreement with mine observations, although indirectly imposed, also indicate reliable output.

Another question is the use of two-dimensional analyses in a three-dimensional world of underground coal mining. Here the long drive of main entries, over three miles, and the extensive mining on both sides of the main entries suggests a tunnel-like geometry amenable to two-dimensional analysis in a vertical cross-section. Depth varies over the main entries because of topography and certainly influences analysis results because greater depth is associated with higher premining stress. Depths ranged to 2,000 ft (600 m) or more. A depth of 1,601 ft (480 m) used in the analyses here is therefore relatively shallow. For this reason, any adverse results

would be of even more concern at greater depth. Thus, an optimistic view is taken using a relatively shallow depth.

Another question concerns the role of cross-cuts that are not seen in a vertical section across the mains and through the pillars between entries. The effect is to produce an optimistic or lower stress in pillars because the additional load transferred to pillars from cross-cuts is not taken into account. An adjustment can be made to increase pillar load (Pariseau, 1981) but this was not done for the sake of analysis clarity. Cross-cuts also lead to greater roof spans at entry intersections with cross-cuts and thus more complex strata flexure in roof and floor, but again this complication was avoided with error on the side of optimism. A threat to roof or floor safety in two-dimensional analysis would indicate a greater threat in a three-dimensional analysis.

Mesh refinement is always a question of interest in any numerical analysis of stress. Large elements average out stress and may mask yielding that would be observed with smaller elements. Large is relative to excavation size. Tabular excavations are very wide compared to height and thus represent a challenge for numerical analysis. A compromise is always necessary between desire for detail and problem size and run time limitations. In any case, a coarse mesh results in optimistic output, lower element stresses and also lower displacements. For example, a roof element 10x10 ft (3.0x3.0 m) over a 20-ft (6 m) wide entry would certainly mask stress concentration in the roof compared with roof elements 1x1 ft (0.3x0.3 m). However, 100 more small elements per large element would be required. If this requirement were extended over the mesh used, more than 17 million elements would be needed, an impractical number for engineering applications.

A more subtle question that arises in “stress analysis” concerns material behavior. A closely related question concerns relationships between laboratory and mine scale rock properties. These questions are of much interest in rock mechanics research for which there is no general consensus and that are well-beyond the scope of this report. An elastic material model was used here as were laboratory rock properties. Strengths were used to compute the limit to a purely elastic response and element safety factors. Generally, rock masses contain discontinuities such as joints and cleats that are absent in laboratory-scale test specimens. Consequently, rock masses tend to be weaker and more compliant than laboratory test results would indicate. The result is an optimistic analysis of stress because the higher laboratory moduli and strengths used lead to smaller displacements and less yielding. If an adverse result is observed using rock properties from laboratory tests, results for the mine would likely be worse.

Inelastic behavior of rock under low confinement is likely to be “brittle” with inelasticity appearing in the form of cracking or “damage”. A falling compressive stress-strain curve is often observed in the laboratory in tests under displacement control past the peak of the curve. Without displacement control, fast, violent failure of the test specimen is likely. While a rising stress-strain curve beyond the elastic limit is strain-hardening, a falling curve indicates “strain-softening”. The first is intrinsically stable, while the latter is unstable. Introduction of strain-softening is likely to make a potentially adverse situation, say, with respect to pillar stress, a catastrophic case. Again, a purely elastic model is optimistic because of the avoidance of complex inelastic behavior that may lead to catastrophic failures.

A potentially important inelastic effect absent in elastic analyses is “caving”. Caving over longwall panels is considered to relieve load on shield supports at the face and on chain pillars in panel entries because the length of a cantilever roof beam immediately above the supports is shortened by tensile failure and thus reduces “weight” on the supports. Caving certainly occurs over longwall panels. How high into the remote roof caving propagates is an open question that is sometimes addressed by rules of thumb or experience in a particular mining district. Strata flexure still occurs above the caved zone and transfers load to pillars remaining. Thick, massive sandstones in roof and floor may transfer load over large spans and if failure ensues, large scale collapse is possible. However, reliable caving models, those that initiate and propagate caving from first principals, are not available, and thus, the question of caving effects is left open.

CONCLUSION

Finite element analysis of barrier pillar mining at Crandall Canyon indicates a decidedly unsafe, unstable situation in the making. This conclusion is based on a two-dimensional elastic analysis of a vertical section transverse to the main entries and parallel longwall panels outside of barrier pillars adjacent to the main entries. Elasticity is the de facto standard model for engineering design of bridges, skyscrapers, concrete dams and similar structures throughout the world. Approximations in the analyses here are generally on the optimistic side, so that an adverse situation evident in output data is likely to be worse. For example, complications such as damage in pillar ribs from locally high stress concentration is ignored. Another example is the neglect of load transfer to pillars from cross-cut excavation that would be in addition to load transfer associated with entry excavation. A relatively shallow depth of 1,601 ft (480 m) was

used; actual depth ranges to 2,000 ft (600 m). No pillar extraction was considered after entry development in the barrier pillars. Transfer of load to the remaining pillars during pillar mining in the barrier pillars would increase stress about the entries and remaining pillars as would consideration of greater depth. Both increase outby the considered analysis section.

Elastic behavior is optimistic because stress may exceed strength in a purely elastic analysis. Thus, if an unsafe condition is inferred from results of an elastic analysis, then caution is certainly indicated. In an elastic-plastic analysis, stresses above strength are relieved by fracture and flow of ground ("yielding"). Reduction of peak stress by yielding is likely to cause the zone of fracture and flow (yield zone) to spread to adjacent ground. Yielding by fracture is accompanied by a sudden loss of strength and is associated with fast failure. Glass breakage is an example of fast failure. Yielding by flow may also be accompanied by reduction in strength ("strain softening") which is also unstable and may to lead to fast failure.

However, yielding by flow may also be slow as loss of strength occurs in time. Unfortunately, time effects in strata mechanics are not well understood. Creep, that is, time-dependent flow, to failure may occur in a matter of minutes, hours, or years. Elasticity may also be delayed, that is, strain may not occur instantaneously with stress. In this regard, there are many mathematical models of time-dependent (rheological) material behavior available for analysis, but reliable calculations for engineering design are problematic. Successful forecasts of time to failure in rock mechanics are rare, if they exist at all. In any event, long-term strength is less than short term strength (determined by laboratory tests) used in elastic analysis here. Again, elastic analysis is optimistic because of the use of higher strength.

A multi-stage mining sequence was followed in the analysis here. Main entries were mined first. A tributary area check on pillar stress confirmed finite element results. Entry roofs, pillars, and floors were well within the elastic limit; no yielding was indicated.

Panel mining on both sides of the main entries was done next. During this stage, displacements were constrained in the finite element model to prevent physically impossible overlap of roof and floor strata at seam level during the panel mining stage. This constraint assisted in achieving reasonable agreement between measured subsidence and finite element results. Results indicated 25% of the barrier pillars yielded, while the remaining portions were near yield. Entry pillar safety factors decreased significantly to 1.3; roof and floor safety factors also decreased but remained in the elastic domain.

Entry mining in the north barrier pillar led to yielding of the remaining portion of this pillar and a significant penetration of yielding into the south barrier pillar. The highest safety factor in any pillar, including main entry pillars was 1.2; the lowest was 0.4. Subsequent entry development in the south barrier caused further yielding. The greatest vertical stress in a rib element was more than nine times the unconfined compressive strength of coal. Extensive zones of strata flexure and tensile yielding were observed in roof and floor. A tributary area calculation of average vertical stress at the conclusion of the last mining stage showed close agreement with finite element results.

The large excess of vertical rib stress over strength indicates a potential for rapid destruction of the rib with expulsion of the broken coal into the adjacent entry. The presence of

thick, strong sandstone in roof and floor strata would reinforce this expectation. The broken coal could fill the entry and perhaps restore some horizontal confinement. If a bulking porosity of 0.25 is assumed, then rib failure would extend 60 ft (18 m) into a rib. The extent of failure into a single rib would be less, if both entry ribs failed. Photographs show entries partially filled with broken coal under intact roof. If bottom coal were left, then floor heave could occur, and similarly, if top coal were left. Failure of either top or bottom coal is a release mechanism of horizontal confinement. Another expectation of large, horizontal motion of rib coal into entries would be evidence of shear slip at contacts between roof and floor sandstones, perhaps in the form of "fault" gouge, that is, finely pulverized coal.

In the opinion of the writer, were these finite element model results available in advance, mining in barrier pillars at Crandall Canyon would not be justified.

REFERENCES

Bathe, K.-L., (1982) *Finite Element Procedures in Engineering Analysis*. Englewood Cliffs, N. J., Prentice-Hall, pp 735.

Desai, C. S., and J. F. Abel (1972) *Introduction to the Finite Element Method for Engineering Analysis*. Van Nostrand Reinhold Co., N. Y., pp 477.

Cook, R. D. (1972) *Concepts and Applications of Finite Element Analysis*. John Wiley & Sons, Inc., N. Y., pp 402.

Jones, R. E. (1994) *Investigation of Sandstone Escarpment Stability in the Vicinity of Longwall Mining Operations*. M. S. Thesis, Department of Mining Engineering, University of Utah.

Obert, L. and W. I. Duvall (1967) *Rock Mechanics and the Design of Structures in Rock*. John Wiley & Sons, Inc., N. Y., pg 490.

Oden, J. T. (1972) *Finite Elements of Nonlinear Continua*. N.Y., McGraw-Hill, pp 432.

Pariseau, W. G. (1981) Inexpensive but Technically Sound Mine Pillar Design Analysis. *Intl. J. for Numerical and Analytical Methods in Geomechanics.* Vol. 5, No. 4, pg 429-447.

Pariseau, W. G. (2007) *Finite Element Analysis of Inter-Panel Barrier Pillar Width at the Aberdeen (Tower) Mine.* Department of Mining Engineering, University of Utah and Bureau of Land Management, Salt Lake City, Utah.

Rao, T. V. (1974) *Two Dimensional Stability Evaluation of a Single Entry Longwall Mining System.* M. S. Thesis, Department of Mining Engineering, University of Utah.

Zienkiewicz, O. C. (1977) *The Finite Element Method* (3rd ed). N. Y., McGraw-Hill, pp 787.